

# A Multimodal Simulation of Electroweak Baryogenesis in the Standard Model

Andrew D. Blaikie and R. Michael Winters, IV

Physics Department, The College of Wooster, Wooster, Ohio 44691, USA

(Dated: July 23, 2010)

The abundance of matter over anti-matter is key to understanding the formation of the universe. One proposed mechanism for this asymmetry is Electroweak Baryogenesis, which hypothesizes that when the Higgs field acquired its vacuum energy and broke electroweak symmetry an abundance of matter over anti-matter was generated. With the Standard Model, aspects of bubble nucleation were examined and modeled using *Mathematica*. The phase transition was sonified using *SuperCollider 3* in order to enhance the simulation. Experimental and theoretical evidence has ruled out Electroweak Baryogenesis in the Standard Model, but this was still used as a basis for the mechanism before moving on to extensions of the Standard Model.

## I. INTRODUCTION

### A. Conditions for Baryogenesis

By current observations the visible universe is practically void of anti-matter on all scales. Anti-matter is known to exist in small quantities and may be created in particle accelerators. However, this persistence of matter is hard to explain with many cosmological models. The abundance of matter was attributed to the initial conditions of the Big Bang for many years. It was not until Andrei Sakharov published three conditions that allowed for Baryogenesis, or a process to create an excess of matter, that physicists began to heavily research this topic. Sakharov required the following conditions be present for baryogenesis to occur:

1. A way to violate baryon number
2. CP-Violation
3. A departure from thermal equilibrium.

Baryon number is defined as the number of baryons minus anti-baryons in the universe (a baryon is made up of three quarks, ex. proton, neutron). Sakharov's first condition requires there be some process that can generate an excess of baryons. CP-Violation, or charge-parity violation is when matter and antimatter do not behave in the same way. If there is not enough CP-Violation the anti-matter process that generates an excess of anti-baryons would occur at the same rate as the process that generates an excess of baryons, thus no imbalance could be formed. Finally, if the universe were in thermal equilibrium, the reverse reactions would occur at the same rate. So a departure from thermal equilibrium is necessary to achieve the matter anti-matter imbalance. All three of these conditions may be applied to the Electroweak Phase Transition. In order to apply these conditions, the dynamics of the phase transition needs to be understood.

### B. The Electroweak Phase Transition

When the universe was very young, it was highly energetic. At these high energies, the electromagnetic and the weak nuclear force were symmetric and mediated by four massless gauge bosons. As the universe cooled, the Higgs field acquired its vacuum expectation value of 246 GeV, leaving the photon massless and giving mass to the  $W^\pm$  and  $Z$  bosons of the weak force. This moment is of particular interest to Baryogenesis. The Higgs field would not acquire its vacuum energy uniformly throughout spacetime. Regions of space where the Higgs field acquires its vacuum energy are known as "bubbles". These bubbles would expand or shrink depending on their radii. This process is called bubble nucleation and it is within the bubble "walls" that Baryogenesis could occur. An example of this process is displayed in Fig. 1.

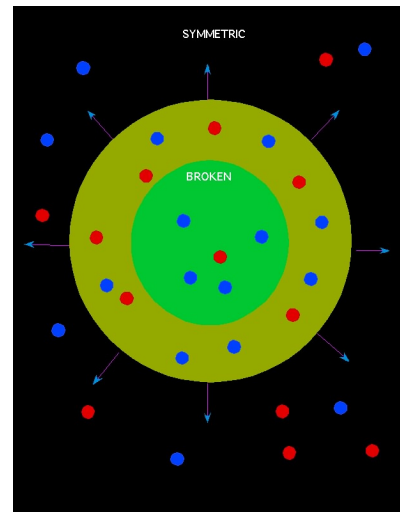


FIG. 1: Bubble Nucleation, blue dots represent baryons while red dots represent anti-baryons. The green represents an area of broken electroweak symmetry and the black represents an area of electroweak symmetry. The yellow represents an area of rapidly changing Higgs field.

### C. Electroweak Baryogenesis

All three of Sakharov's conditions may be applied to the Electroweak Phase Transition. The walls of these bubbles are regions of space where the energy of the Higgs field is rapidly fluctuating. Theoretical research has been done on baryon number violating processes and such a process is possible within the walls. A toy example is shown to demonstrate the ideas behind the theory. Suppose the process to generate an excess of baryons is  $X \rightarrow Y + B$ . If there is enough CP-Violation in the model then this process may occur more often than its anti-matter equivalent process  $\bar{X} \rightarrow \bar{Y} + \bar{B}$ . If the phase transition is significantly first order, or extremely abrupt, the region of rapidly changing Higgs field would be out of thermal equilibrium. Hence the reverse processes  $\bar{Y} + \bar{B} \rightarrow \bar{X}$  and  $Y + B \rightarrow X$  would not occur at the same rate as the forward processes, perpetuating the imbalance. The excess of baryons would be swept into the bubble and acquire mass. Since the new conditions are drastically different inside the bubble, the excess matter would persist and baryon number would be violated. Fig. 1 shows how more matter may be swept inside the bubble through these processes.

However, the Standard Model does not provide enough theoretical CP-Violation for this process to generate the observed excess of matter. Also, the mass of the Higgs boson would have to be less than roughly 40 GeV to create a large enough departure from thermal equilibrium[1]. If that were the case, particle accelerators would have already discovered the particle. Other models such as Supersymmetry or the Two-Higgs Doublet Model may allow for more CP-Violation and possibly a higher Higgs mass. Thus, Electroweak Baryogenesis is not ruled out in those models.

This paper will simulate Bubble Nucleation within the Standard Model. A Higgs mass of 35 GeV will be assumed. Even though this is unphysical, it will help demonstrate the ideas of Electroweak Baryogenesis. Without presenting the full derivation, this paper provides the equations necessary for a simulation.

## II. EFFECTIVE POTENTIAL

All of the equations necessary for the effective potential are taken from [1]. The effective potential is used to show the Higgs field's tendency to change with decreasing temperature. Specifically, the effective potential of the Higgs Field is dependent upon its energy  $\phi$  and temperature  $T$  and may be modeled by

$$V(\phi, T) = d(T^2 - T_o^2)\phi^2 - eT\phi^3 + \frac{\lambda_T}{4}\phi^4, \quad (1)$$

where

$$\begin{aligned} d &= \frac{2m_t^2 + 2m_w^2 + m_z^2}{8v_o^2}, \\ e &= \frac{2m_w^3 + m_z^3}{4\pi v_o^3}, \\ b &= \frac{3(2m_w^4 + m_z^4 - 4m_t^4)}{64\pi^2 v_o^4}, \\ T_o^2 &= \frac{m_h^2 - 8bv_o^2}{4d}. \end{aligned}$$

Also,

$$\begin{aligned} \lambda_T &= \lambda - \frac{3}{16\pi^2 v_o^4} \left( 2m_w^4 \left[ \ln\left(\frac{m_w^2}{T^2}\right) - \ln(ab) \right] \right. \\ &\quad \left. + m_z^4 \left[ \ln\left(\frac{m_z^2}{T^2}\right) - \ln(ab) \right] \right. \\ &\quad \left. - 4m_t^4 \left[ \ln\left(\frac{m_t^2}{T^2}\right) - \ln(af) \right] \right), \quad (2) \end{aligned}$$

where  $\ln(ab) = 3.91$  and  $\ln(af) = 1.14$ . The Higgs quartic coupling constant is  $\lambda = \frac{m_h^2}{2v_o^2}$ .  $m_t$ ,  $m_w$ ,  $m_z$ , and  $v_o$ , are the mass of the top quark, the  $W^\pm$  boson, the  $Z$  boson, and the Higgs vacuum expectation value, respectively.

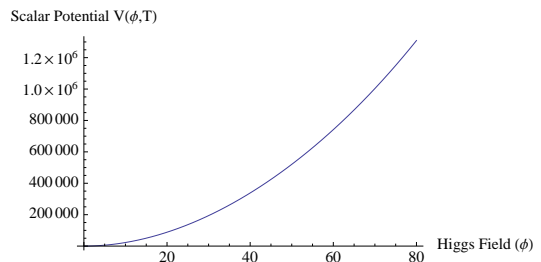


FIG. 2: The effective potential for Higgs Mass 35 GeV and 80 GeV Temperature.

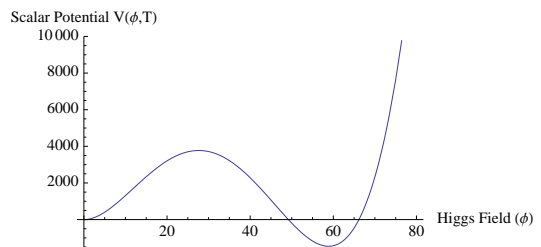


FIG. 3: The effective potential for Higgs Mass 35 GeV and 71.4 GeV Temperature.

To better understand the effective potential, another toy example is useful. Consider the effective potential  $V$  to be a potential energy function where the Higgs field is a ball with some predefined kinetic energy. At high temperatures the potential energy field looks like Fig. 2, where the ball tends to roll down towards the origin. But as the universe cools, the graph begins to form a second

minimum as can be seen in Fig. 3. Now the ball with kinetic energy might roll into the degenerate minimum and not have enough kinetic energy to leave. This process explains how a bubble would form. The Higgs field would go through an abrupt change as it rolls over the hill, so the transition to its vacuum energy would be first order, which is necessary for a sufficient departure from thermal equilibrium.

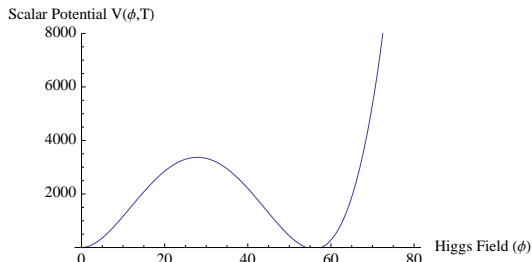


FIG. 4: The effective potential for a Higgs mass of 25 GeV at its critical temperature.

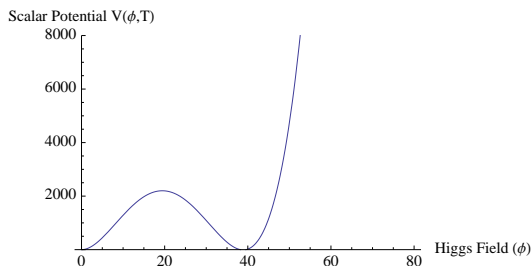


FIG. 5: The effective potential for a Higgs mass of 90 GeV at its critical temperature.

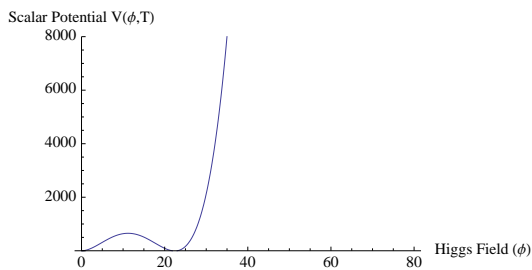


FIG. 6: The effective potential for a Higgs mass of 150 GeV at its critical temperature.

It has been mentioned that in the Standard Model, a light Higgs mass is needed to achieve a large enough departure from thermal equilibrium. This may be shown by plotting different Higgs masses at the critical temperature, the point when the degenerate minimum has the same effective potential value as the origin.

Figs. 4, 5, and 6 show the effective potential at its critical temperature. Notice that as the Higgs mass increases the position of the 2nd minimum decreases. From this we can conclude that the phase transition is becoming less

abrupt and thus the departure from thermal equilibrium is weaker.

The equations for the effective potential are necessary for a model of bubble nucleation because they are used to derive the critical radius where the bubble either shrinks or grows depending on its initial radius. Since the simulation will assume a Higgs mass of 35 GeV, the critical temperature will be needed for that Higgs mass. This was found to be  $T_c = 71.4189$  GeV.

### III. CRITICAL RADIUS AND WALL VELOCITY

To create the simulation, one must derive values for the critical radius and wall velocity of the bubbles. The critical radius of a nucleating bubble is determined by the energy gained within the bubble. Recall the effective potential toy example. If the ball rolled into the degenerate minimum but still had enough kinetic energy to roll back to the stable minimum, there would have been a brief time when Electroweak Symmetry was broken. This process explains how a bubble might form but then shrink because the energy gained was not enough for the bubble to grow. The critical radius equations are defined in [3].

In order to determine the energy of a given bubble, and then derive the critical radius, begin with the equation

$$E(r) = 4\pi\sigma r^2 - \frac{4}{3}\pi\Delta V r^3, \quad (3)$$

where  $r$  is the radius,  $\sigma$  is the “surface tension” and  $\Delta V$  is the difference in the effective potential between the stable minimum and the degenerate minimum. In order to find  $\Delta V$  the first derivative of the effective potential was taken with respect to  $\phi$ . The non-zero answer with a positive second derivative was set equal to zero and solved for  $\phi$ . This value was calculated to be

$$\phi_{t_c} = \frac{0.5(3eT + \sqrt{q})}{\lambda_T}, \quad (4)$$

where

$$q = 9e^2T^2 - 8dT^2\lambda_T + 8dT_o^2\lambda_T. \quad (5)$$

$\Delta V$  can now be solved by using  $\phi_{t_c}$  in the effective potential,

$$\Delta V = V(\phi_{t_c}, T). \quad (6)$$

The surface tension is found in reference [2]:

$$\sigma = \frac{\phi_c^2}{L_w}, \quad (7)$$

where  $\phi_c = \frac{(2eT_c)}{\lambda_{T_c}}$  and  $L_w = \frac{1}{\sqrt{d(T^2 - T_o^2)}}$ . In this case  $L_w$  is the wall width and  $T_c$  is the critical temperature.

From equation 3 the point where the change in energy is zero can be found. This point is the critical radius:

$$r_c = \frac{2\sigma}{\Delta V}. \quad (8)$$

This point is further illustrated in Fig. 7.

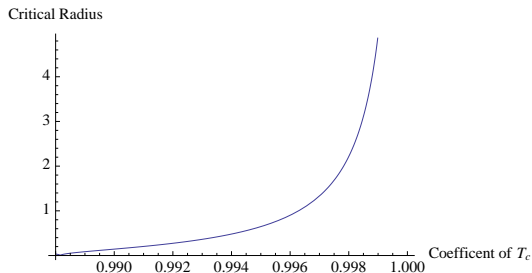


FIG. 7: The critical radius plotted with temperature. It can be seen that as the temperature decreases the critical radius also decreases.

The derivation for the wall velocity was found in [4]. The values from Table I were interpolated on Mathematica in order to find a value for a Higgs mass of 35 GeV. The wall velocity was approximated to be  $V_w = 0.375 * c$ , where  $c$  is the speed of light. This value was incorporated into the simulation.

TABLE I: Wall Velocity

Higgs mass (GeV)	Wall Velocity (c)
0	0.365
34	0.374
50	0.392
70	0.412
81	0.428
91	0.441

#### IV. PROBABILITY FUNCTIONS

Now that the critical radius and wall velocity have been defined, the probability of bubble formation at a particular time, and the initial radius of a bubble are also needed for the simulation.

##### A. Determining Initial Radius

To determine the initial size of a bubble, a generic approximation of bubble nucleation was applied to the Electroweak Phase Transition. The probability function as defined in [5] is

$$P_r(T, y) = y^{-\gamma(T)}, \quad (9)$$

where

$$\begin{aligned} \gamma(T) &= a_2 \lambda_i(T)^2 - a_1 \lambda_i(T) + a_o, \\ \lambda_i(T) &= \sqrt{\frac{4\pi\sigma}{T}} r_c, \\ a_1 &= 0.005, \\ a_2 &= 0.093, \\ a_o &= 0.02. \end{aligned}$$

and  $y$  is the ratio of  $\frac{r}{r_c}$ . If the ratio is greater than 1 the bubble grows; if it is less than one the bubble shrinks.

When the function is plotted, the area under the curve represents the probability that a bubble will be formed within the corresponding domain. We note that the function is also temperature dependent so the distribution of bubbles will not be uniform with time. Fig. 8 shows the probability function near the start of the phase transition. A higher probability is given for a bubble to shrink in this case. However, as the temperature cools the function gives equal probabilities for radii sizes as seen in Fig. 9.

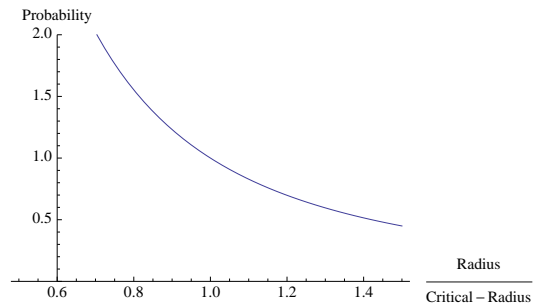


FIG. 8: The probability of the initial radius, plotted with a temperature equal to 0.99 of the critical temperature.

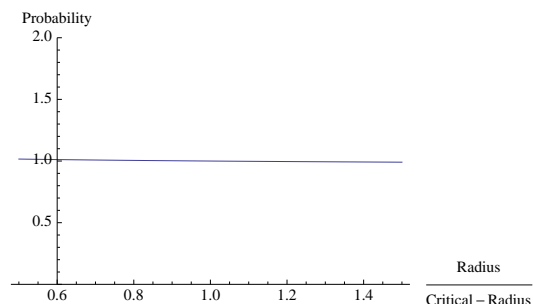


FIG. 9: The probability of the initial radius, plotted with a temperature equal to 0.9882 of the critical temperature.

##### B. Determining Formation Time

Next, a function to determine the probability for a given bubble to form with respect to time was determined. As the universe evolves, it also cools, so time is

related to temperature. An approximation for the probability of formation time was found in [6]. The function

$$P_t(T) = e^{-S(T)}, \quad (10)$$

where  $S(T) = \frac{S_3(T)}{T}$ ,

$$S_3(T) = \frac{16\pi}{3} \frac{\sigma^3}{\left(L(T) \left[1 - \frac{T}{T_c}\right]\right)^2}, \quad (11)$$

and

$$L(T) = 4 \frac{\Delta V}{\left(1 - \frac{T^4}{T_c^4}\right)}, \quad (12)$$

will be used.

This probability function works the same way as  $P_r$  of eq. 10 in the way of determining the probability of a particular domain. By examining Fig. 10, it can be seen that bubbles are more likely to form near the end of the phase transition. Also, that the real values of Fig. 10 are the same as the changing temperature between Figs. 8 and 9.

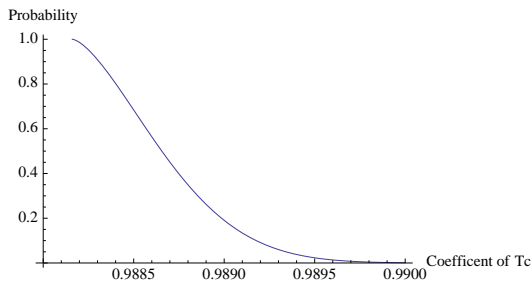


FIG. 10: The probability a bubble is formed vs. Temperature. Values before 0.9882  $T_c$  were complex.

## V. PROGRAMING THE SIMULATION

The goal of this simulation was to demonstrate how these bubbles might form and grow over a certain area of space and time.

### A. Scaling Space and Time

In order to have a physical simulation the correct scaling for space and time had to be determined. For scaling time and temperature, the domain of the real values for  $P_t$  was used. These ranged from 0.99  $T_c$  - 0.9882  $T_c$ . This was then converted to a 10 second time scale.

A way to establish the spacing of the bubbles will be needed for the simulation. From [6], the equation

$$r_s = (8\pi)^{1/3} V_w t_g, \quad (13)$$

will give the average spacing between a bubble and the nearest bubble.  $V_w$  is the wall velocity and the growth temperature is

$$t_g = t_c \frac{0.489}{2\text{Ln} \left[ \frac{(m_p)^4}{T_c^4} \right]^{3/2}}, \quad (14)$$

where  $t_c$  is the time at the critical temperature and  $m_p$  is the Plank mass. An approximation for a temperature to time conversion may be found in [3]. The conversion

$$t = (1000T)^{-2}, \quad (15)$$

was used.

For  $r_s$  to be used, the average spacing between a given bubble and its nearest bubble had to be found in the case of the simulation. Thirty bubbles were programed to form within a 300 x 300 unit, 2 dimensional space. A program was written, and the average spacing was found to converge to 29.7 units.

### B. Generating Parameters

The next step was to program how to determine the parameters for a given bubble. These include:

- I.) X and Y coordinates,
- II.) Formation time of the bubble,
- III.) Initial radius,
- IV.) Check for overlap.

The X and Y coordinates for each bubble were chosen with no weights. This proved to be the simplest method and since thirty bubbles were used, an even distribution often followed.

The formation time of a given bubble was weighted by  $P_t$ . In order to weight the probability properly, the ‘RandomChoice’ Mathematica command was used. Two lists are required for this command, the first being a list of probabilities and the second being a list of outputs. The first element in the probability list corresponded to the first element on the output list. It proved easiest to use the height of  $P_t$  at a given temperature to correspond directly with that coefficient of  $T_c$ . Using arrays, 1000 elements were generated for each list and a weighted formation time could be found.

To determine the initial radius  $P_r$ , was implemented. However, unlike  $P_t$ ,  $P_r$  is dependent on temperature in addition to its domain values. To account for this, the program evaluated all of the formation times first. Then these thirty values were entered into thirty  $P_r$  functions to create 30 distinct probability functions. From these, the ‘RandomChoice’ command was used the same way as determining the formation time. Arrays of 1000 probabilities corresponded to 1000 initial radii and a properly weighted radii size was outputted. The ‘If’ command was used to cause radii less than one to shrink.

Next, an algorithm to reject bubbles that would form overlapping with other bubbles was written. After much experimentation, the method implemented used arrays to keep track of space with broken symmetry. The thirty start times were arranged from first to last by the ‘Sort’ command. A 1 was assigned to bubbles that could form and 0 to bubbles that would form inside another. The first bubble was given a one automatically. When the second bubble formed the array process began. A 300 x 300 array was evaluated for the first bubble at the formation time of the second bubble. Using a combination of ‘If’ commands and the distance formula, a 1 was given to an element of the array that a bubble occupied and a 0 was assigned to elements of electroweak symmetry. The next 300 x 300 array used the same process, but only used the incoming bubble. Next, the two arrays were added together. If the second bubble formed inside the first bubble a 2 would appear in some element of the new array. To determine if any 2s were present an ‘If’ statement set the new array equal to itself squared. If the equation evaluated to be true the new bubble was allowed to form. This process was repeated each time a bubble was formed. The first array in the sequence used all of the relevant previous bubbles and the second array only used the incoming bubble.

After all of the parameters were calculated, they were exported to be simulated. The parameter set next was manipulated to the necessary format for sonification and then exported in the form of .csv files for the sonification process.

## VI. SONIFICATION

In order to enhance the simulation, a sonification was created using the program *SuperCollider 3*[7]. Two synthesis definitions were employed, one to represent the formation of the bubbles over time, the other to represent the amount of space that still had Electroweak Symmetry. The sonification techniques employed were judged to be effective based upon brief discussions of auditory perception with Dr. Neuhoff and Dr. Walker in 2009, various papers from the ICAD proceedings [8], and the current understanding of SuperCollider.

### A. Sonification of Bubble Formation

The sonification of bubble formation was modeled upon three known quantities,

- A) the time that the bubble first appeared,
  - B) its horizontal (X) position, and
  - C) its vertical (Y) position,
- (16)

as generated using the previously described Mathematica notebook. Mathematica exported these values into a .csv file on the hard drive where they were imported using

SuperCollider. Using A from (16), two additional values were derived,

- D) time until the end of the simulation, and
  - E) time between bubble events.
- (17)

An example data set imported into SuperCollider is displayed in Table II.

TABLE II: An example data set imported into SuperCollider for a 13 second simulation. A, B, C, D and E refer to the titles in (16) and (17). The values for A, D, E are in seconds and C, D are the relative X and Y positions on a 300 x 300 visual grid.

Bubble #	A	B	C	D	E
1	5.6	23.44	73.45	7.4	0.53
2	6.13	254.97	91.67	6.87	1.79
3	7.92	193.55	40.59	5.08	0.08
4	8	172.75	151.04	5	0.06
5	8.06	89.96	183.79	4.94	0.71
6	8.77	161.62	65.08	4.23	0

In previous sections, it was mentioned that each bubble that formed had an initial radius  $r$  that would shrink or grow depending upon its magnitude. Values for  $r$  that were below some critical radius  $r_c$  would briefly appear and then disappear, whereas cases with  $r > r_c$  described all bubbles which lasted until the end of the simulation. The bubbles which quickly shrank were not sonified because of lack of time and because a sufficient technique for sonification was not determined. However, because instances of shrinking bubbles ( $r < r_c$ ) were so perceptually insignificant compared to the bubbles which expanded ( $r > r_c$ ), our choice was not thought to take away from the overall simulation.

#### 1. Spatialization, Pitch, Timbre

Auditory parameters for bubble formation were chosen in such a way as to minimize perceptual interference between parameters and maximize aesthetic appeal. For this purpose, Spatialization, Timbre, Intensity and Pitch were the auditory parameters chosen for representation.

For every bubble  $r > r_c$  there was one corresponding sound event such that the bubble’s X-position corresponded to horizontal spatialization, its Y-position corresponded to pitch (high Y-position  $\rightarrow$  high pitch), and the increasing radius corresponds to a timbre and intensity which changes in a way intended to simulate the feeling of expansion.

In SuperCollider, spatialization was controlled using ‘Pan2’, a two channel equal power panner function. Pitch was controlled using ‘Midicps’, a command which converts MIDI notes to their corresponding frequency. The MIDI range used in the present sonification was 40-60 or

alternatively, E2 to C4 in musical notation. Timbre was controlled using ‘Formant,’ a command which generates a set of harmonics around a formant frequency given a certain fundamental frequency. Both the formant frequency and the pulse width frequency increased from 100-1000 Hertz along an exponential curve (‘XLine’) in the time frame of D-1 seconds. D-1 refers to the first element of the D column in Table II. Only the first bubble reaches the 1000 Hz level.

So that the sonification would outlast the Electroweak Phase Transition, an extra three seconds were added to the simulation. This additional time created a fuller auditory experience. Because the data was not generated for a 13 second visualization, only visualizations in which the entire visual grid had undergone transition after 10 seconds were deemed physical. The majority of the visualizations did not complete the phase transition within 10 seconds, consistent with [6].

## 2. Intensity

The intensity of a bubble forming was also varied over time such that the increasing bubble size would have an analogous auditory experience. In SuperCollider, the Envelope Generator (‘EnvGen’) was used to control the intensity over time. An example envelope is displayed in Fig. 11. The envelope was designed such that every bubble could be heard when it first entered, but by the end of the simulation, would not be as loud as the bubble which began before it. By making the intensity increase or decrease cubically, we are reminded that the volume of a bubble does not increase linearly with respect to  $r$ . Though the volume increases proportionally to  $r^2$  not  $r^3$ , this relationship was overlooked.

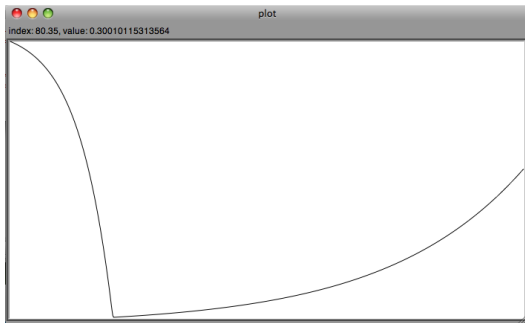


FIG. 11: An example envelope for controlling the intensity over time of each bubble. This envelope corresponds to Bubble #4 of Table II. The initial intensity of 1 decreases to 0.3 cubically in the 1 time frame of second. Having reached its minimum value it approaches its final intensity of 5/7.4 cubically in the time frame of 5-1 seconds. Note that the entire envelope occurs over the time frame of D-4 of Table II.

While designing the sonification, it was determined that bubbles with lower pitch (lower Y-coordinate), sounded softer than higher pitch bubbles (higher Y-

coordinate). Though it was not known the exact relationship for perceived equal intensity across octaves, an additional intensity function was created to compensate for this inequality. The function was constructed so that the amplitude of the lowest possible pitch (E2) was twice that of the highest possible pitch (C4), with a linear relationship between the endpoints. For the simulations analyzed, this additional function was thought to be perceptually sufficient.

## B. Sonification of Electroweak Symmetry

In sonifications that involved only bubble formation, about the first five seconds of the simulation are completely silent. However, we are reminded that before electroweak symmetry breaking, though the universe was massless, it was surging with energetic particles streaming at the speed of light. Silence during this portion of the simulation was thought to be misleading and was jettisoned; replaced by a more appropriate sound.

After brief experimentation with the Unit Generators available in SuperCollider, a crackling noise was chosen for the area which had not yet undergone transition. In SuperCollider, this crackling noise was generated using ‘Dust2’, a function which generates a certain density of random impulses from -1 to 1. The average number (density) of these random impulses per second was chosen to be a constant 1000.

As bubbles are formed, the area which still has electroweak symmetry slowly decreases. For this period of time, the intensity of the dust decreases proportional to the amount of space that still has electroweak symmetry. As in section VIA, the Envelope Generator ‘EnvGen’ was used for its control of intensity. An example envelope can be viewed in Fig. 12.

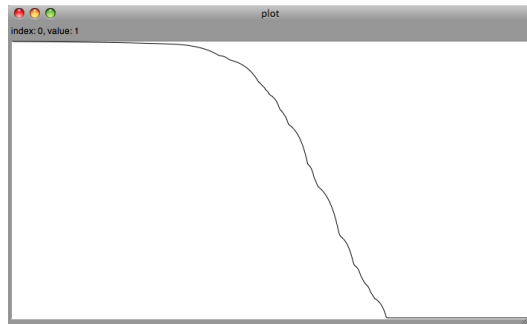


FIG. 12: A screenshot from SuperCollider displaying the envelope of ‘Dust2’ over a period of 13 seconds. Beginning with an initial intensity of 1, as electroweak symmetry is broken the envelope decreases to a final value of 0 when electroweak symmetry is completely broken.

The envelope was created using the arrays generated in section VB that determined whether bubbles would form inside other bubbles. Though more rigorous calculations could be employed to calculate this area over time,

they were not attempted because of lack of time. Furthermore, the perceivable difference in sound between the two methods was not thought to be substantial enough to merit further inquiry.

### C. Conclusions and Future Work

The sonification created to model electroweak symmetry was thought to be effective because it communicated the necessary information and had an additional aesthetic appeal. Its effectiveness was confirmed by instances in which errors in the *Mathematica* code were discovered through sonification. Additionally, instances in which the visualization and sonification were not of the same data set were easily perceived.

Several issues involving the intensity of the sound files arose. It was discovered that lower pitches were softer than higher pitches despite being equal in all other respects. A better understanding of perceived intensity across octaves could lead to a better sonification.

Though the envelope of Fig. 11 gave special emphasis to bubbles that had just formed, at some points it proved insufficient in this respect. There were instances in which new bubbles were not heard as clearly as others because of the intensity of the combined sounds of other bubbles which had previously formed. Though perhaps these new

events are less relevant when there are many bubbles expanding simultaneously, perhaps a different envelope in Fig. 11 would better.

Physically speaking, at the phase transition, the total amount of energy in the universe does not cool drastically. While the sonification effectively demonstrated the phase transition, the intensity of the dust sound is not as great as the intensity of the sounds after the transition. This discrepancy could be misleading and should be altered to keep a constant intensity over time.

Another option for displaying the amount of electroweak symmetry over time would be altering the density of ‘Dust2’ over time instead of its intensity. Although this possibility was considered, it required curve fitting in SuperCollider, a task for which SuperCollider was not thought capable.

### VII. ACKNOWLEDGMENTS

We would like to thank Dr. Deva O’Neil for her motivation and guidance in giving us an introduction in particle physics. Her excitement to develop a multimodal simulation of bubble nucleation proved to be very helpful. This research was supported by the NSF-REU grant DMR-0649112 and the College of Wooster.

- 
- [1] M. Dine, arXiv:hep-ph/9206220.
  - [2] A. Megevand and A. D. Sanchez, Nucl. Phys. B **825**, 151 (2010) [arXiv:0908.3663 [hep-ph]].
  - [3] D. Boyanovsky, H. J. de Vega and D. J. Schwarz, Ann. Rev. Nucl. Part. Sci. **56**, 441 (2006) [arXiv:hep-ph/0602002].
  - [4] G. D. Moore and T. Prokopec, Phys. Rev. D **52**, 7182 (1995) [arXiv:hep-ph/9506475].
  - [5] L. V. Bravina and E. E. Zabrodin, Phys. A, 202 (1995).
  - [6] K. Enqvist, J. Ignatius, K. Kajantie and K. Rummukainen, Phys. Rev. D **45**, 3415 (1992).
  - [7] <http://supercollider.sourceforge.net>
  - [8] <http://www.icad.org/conferences>